Final accepted manuscript.
Published in the Journal of Mass Spectrometry, 2021, Volume 56, Issue 1, e4693, John Wiley & Sons, Inc.
https://doi.org/10.1002/jms.4693

Collision energies on QTof and Orbitrap instruments: How to make proteomics measurements comparable?

*Dániel Szabó,[1,2)] Gitta Schlosser,[3)] Károly Vékey,[1)] László Drahos,[1)] Ágnes Révész[*1)]*

[1)] MS Proteomics Research Group, Research Centre for Natural Sciences, Magyar Tudósok körútja 2., H-1117, Budapest, Hungary

[2)] Hevesy György PhD School of Chemistry, ELTE Eötvös Loránd University, Faculty of Science, Institute of Chemistry, Pázmány Péter sétány 1/A, H-1117, Budapest, Hungary

[3)] MTA-ELTE Lendület Ion Mobility Mass Spectrometry Research Group, Eötvös Loránd University, Faculty of Science, Institute of Chemistry, Pázmány Péter sétány 1/A, H-1117, Budapest, Hungary

KEYWORDS: collision energy, Orbitrap, QTof, bottom-up proteomics, similarity index

ABSTRACT. QTof CID and Orbitrap HCD are the most commonly used fragmentation techniques in mass spectrometry based proteomics workflows. The information content of the MS/MS spectra is first and foremost determined by the applied collision energy. How can we set up the two instrument types to achieve maximum transferability? To answer this question, we compared MS/MS spectra obtained on a Bruker QTof CID and a Thermo Q-Exactive Focus Orbitrap HCD

instrument as a function of collision energy using the similarity index. Results show that with a few eV lower collision energy setting on HCD (Orbitrap-specific CID) than on QTof CID, nearly identical MS/MS spectra can be obtained for leucine enkephalin pentapeptide standard, for selected +2 and +3 enolase tryptic peptides and for a large number of peptides in a HeLa protein digest. The Bruker QTof was able to produce colder ions, which may be significant to study inherently labile compounds. Further, we examined energy dependence of peptide identification confidence, as characterized by Mascot scores, on the HeLa peptides. In line with earlier QTof results, this dependence shows one or two maxima (unimodal or bimodal behavior) on Orbitrap. The fraction of bimodal peptides is lower on Orbitrap. Optimal energies as a function of m/z show a similar linear trend on both instruments, which suggests that with appropriate collision energy adjustment, matching conditions for proteomics can be achieved. Data has been deposited in the MassIVE repository (MSV000086434).

INTRODUCTION

Tandem mass spectrometry has become a widely used analytical tool in the investigation of small molecules as well as in proteomics. The applied methods involve various fragmentation techniques differing in the mode of activation, *e.g.,* collision induced dissociation (CID) or electron transfer dissociation (ETD).[1–3] In the case of the most frequently used CID, spectrum characteristics are mainly influenced by energetics (like low and high energy CID), by the timescale and the number of collisions (like quadrupoles or ion traps), but also depend on instrumentation (like triple quadrupole – QQQ or quadrupole time-of-flight – QTof) and on experimental conditions. Collision energy is the parameter most often varied in CID MS/MS; its choice materially affects spectrum quality and usefulness. At low internal energy, the precursor ion is the most abundant peak in the

spectrum, while at high internal energy it may be completely fragmented. The relative intensity of various fragment ions also change significantly as a function of energy.

In bottom-up proteomics, proteins in a sample are identified via digesting them into a mixture of peptides and analyzing the result via LC-MS/MS. The resulting MS/MS spectra are linked to peptide sequences based on the characteristic peptide fragment ions, either using a sequence database or "*de novo*". Peptide fragmentation and its collision energy dependence have been extensively studied and reviewed,[4–7] but the efficiency of MS-based bottom-up proteomics workflows received much less attention.

Recently, we have studied collision energy effects in a large scale proteomics study using a QTof mass spectrometer, which is one of the most frequently used instrument in this field.[8] We have characterized the quality of a CID spectrum by the identification score of the database search using the widely accepted Mascot search engine. For some peptides, it has been found that the Mascot score as a function of the collision energy showed an approximately Gaussian profile, with about 10 eV width at half-maximum ("unimodal behavior"). Surprisingly, for more than half of the peptides, the Mascot score vs. collision energy curve does not show a single, well-defined optimum; rather, it has two distinct maxima or at least a broad plateau implying the presence of two peaks close to each other ("bimodal behavior"). This phenomenon is linked to the different energy dependence of *b* and *y* fragment ions[7]. The *b* ions' intensity shows maximum at the lower energy optimum, while *y* ions are most abundant at the higher energy maximum, although the latter are dominant in the whole energy range. These findings led us to develop novel proteomics workflows via energy optimization, resulting in significantly better protein coverage, higher sequence coverage[8,9] and more efficient sequence validation[10] than typical protocols using generic collision energy setup.

QTof instruments have been the method of choice in many areas, but Orbitraps are becoming the most widespread technique for a number of analytical purposes. Orbitraps/HCD cells and QTofs show high degrees of similarity in terms of fragmentation,[11,12] and they are usually handled as equivalent methods even though the literature lacks detailed and systematic comparative studies, and some differences have been pointed out.[13] Orbitraps were found to be comparable or even outperform QTof in the analytical characterization of small molecules in various contexts (metabolomics, drugs, etc.),[14–20] as well as in the identification and quantification of proteins using both bottom-up and intact methods.[21–25] Studies of peptide fragmentation in HCD cells, the appropriate choice of experimental parameters used in proteomics, and studies on the transferability of results and experimental setup between the two instruments are all of significant importance.

Recently, we have developed a methodology for the comparison of different instrument types by adopting a measure of spectrum similarity. This allows finding the collision energy in one instrument that produces the most similar spectrum to that obtained at a given collision energy on another instrument.[26] The results showed that at low collision energies (when the precursor was the most abundant peak in the spectrum) it was possible to obtain very similar (similarity > 0.99) spectra on QQQ, QTof, and ion trap instruments by appropriate collision energy settings. At medium and at high collision energy (when the precursor ion was mostly or completely fragmented), closely similar spectra could still be obtained on QQQ and QTof. On the ion trap instrument, however, it was impossible to generate a similar spectrum, and differences increased with increasing collision energy. Notably, Orbitrap/HCD was not included in this study of ours. These results are in line with the generally accepted view on the difference on the ion excitation mechanism. In particular, ion traps selectively energize parent ions, while in QQQ, QTof, and

Orbitrap/HCD instruments, excitation of all species can open up more parallel and consecutive reaction channels.[27–31]

In the present work, we extend our investigations to the similarity of QTof and Orbitrap instruments to understand how we can provide comparable and transferable methodologies on these two key instruments. First, we compare collision energy effects on these two, widely used instrument types, using the HCD cell on the Orbitrap. Detailed analysis is performed on leucine enkephalin, which is a small, mass spectrometric reference peptide.[32] Subsequently, we move on to tryptic peptides by investigating two doubly and two triply charged species from enolase digest standard as representative examples. Finally, we examine the transferability of the conclusions on energy dependence of proteomics identification confidence and that of the collision energy optimization strategy from QTof to Orbitrap equipment. To this end, we carry out systematic energy dependent LC-MS/MS measurements on a large set of peptides from a complex proteomic standard (HeLa tryptic digest) and use our in-house developed software to identify optimum energies, trends, and spectral similarity. Our findings prove that QTof and Orbitrap instruments deliver equivalent data quality for MS-based proteomics if a little extra care is taken to adjust collision energies.

EXPERIMENTAL SECTION

Chemicals and Reagents

LC-MS grade solvents and leucine enkephalin (amino acid sequence is YGGFL) were purchased from Sigma Aldrich (Sigma-Aldrich Kft., Budapest, Hungary), while HeLa tryptic digest standard was obtained from Thermo Fisher Scientific (Thermo Fisher Scientific, Waltham, MA, USA). MassPREP enolase digest standard was from Waters (Waters, Milford, MA, USA).

Mass Spectrometry Analysis

Experiments were carried out using a Bruker Maxis II ETD QTof (Bruker Daltonics, Bremen, Germany) and a Q-Exactive Focus Orbitrap (Thermo Fisher Scientific, Waltham, MA, USA) mass spectrometer.

Leucine enkephalin and tryptic peptides from enolase. The fragmentation of leucine enkephalin (amino acid sequence: YGGFL) was investigated in positive electrospray ionization mode. The protonated molecule was generated by spraying a 0.5 ng/µl solution in 1:1 water:acetonitrile + 0.1% formic acid (FA) with a flow rate of 10 µl/min. Tryptic enolase peptides were measured from 200 fm/µl solution in 1:1 water:acetonitrile + 0.1% FA with a flow rate of 5 µl/min. Two doubly charged peptides (NVNDVIAPAFVK^{2+} and AVDDFLISLDGTANK^{2+}) and two triply charged peptides (TAGIQIVADDLTVTNPK^{3+} and SIVPSGASTGVHEALEMR^{3+}) were mass-selected and examined. The ESI source conditions for Bruker Maxis II ETD were as follows: capillary voltage 4500 V, temperature 180°C, end plate offset -500 V, dry gas 4.0 L/min and nebulizer 0.4 bar. For the Thermo Orbitrap mass spectrometer, the following ESI source parameters were applied: the spray voltage was 4 kV, spray temperature was set to 320°C, while the sheath and auxiliary gas flows were kept at 5 and 3 arbitrary units, respectively.

For leucine enkephalin, mass-selected singly protonated molecules were collided by nitrogen gas using various collision energy values. For the Bruker equipment, CE range from 0 to 100 eV was mapped in steps of 2 eV (0-10 eV and 30-40 eV range), in steps of 1 eV (10-30 eV range) and in steps of 5 eV (40-100 eV range). In the case of Thermo Orbitrap instrument, collision energy was varied from 10 eV to 80 eV in steps of 1 eV (10-20 eV range), in steps of 2 eV (20-30 eV range) and in steps of 5eV (30-80 eV range).

The MS/MS spectra of doubly and triply protonated enolase peptides were investigated at CE values ranging from 5-50 eV in steps of 2-5 eV on the Bruker mass spectrometer. In the case of the Thermo Orbitrap equipment, CE was varied between 11 and 50 eV, again in steps of 2-5 eV.

HeLa tryptic digest standard. Collision energy dependent nano-LC-MS/MS measurements of HeLa tryptic digest on the Bruker Maxis II ETD QTof instrument were recorded earlier as part of a previous work on the Mascot score – collision energy relationship.[8] The detailed description of the experiments can be found in the previous publication, therefore only a brief summary is presented here. In each run, 50 ng HeLa was subjected to nano-LC-MS/MS analysis using a Dionex Ultimate 3000 RSLC nano-LC coupled to the mass spectrometer. Sample was injected onto an Acclaim PepMap100 C18 trap column (5 µm, 100 Å, 100 µm × 20 mm, Thermo Fisher Scientific, Waltham, MA, USA) and peptides were separated on an Acclaim PepMap RSCL C-18 analytical column (2 µm, 100 Å, 75µm × 500mm, Thermo Fisher Scientific, Waltham, MA, USA) at 48°C using a flow rate of 270 nL/min. The gradient was as follows: 4% B from 0 to 11 min, followed by a 90 min gradient to 50% B, then the concentration of the solvent B was elevated to 90% in 1 min and kept there for 5 min; solvent A was 0.1% FA in water, while solvent B was 0.1% FA in acetonitrile. Sample ionization was achieved in the positive electrospray ionization mode via a CaptiveSpray nanoBooster ion source. The capillary voltage was set to 1300 V, the nanoBooster pressure was 0.2 bar, the drying gas was heated to 150 °C, and the flow rate was 3 l/min. Spectra were collected using a fixed cycle time of 2.5 s and the following scan speeds: MS spectra at 3 Hz, MS/MS at 16 Hz. In order to limit run-to-run variability of DDA measurements, an increased intensity threshold of 100 000 was used. An active exclusion of 2 min after one spectrum was used, except if the intensity of the precursor was elevated 3-fold. In this data set, collision energies applied to fragment the peptides were chosen to be the sum of an m/z-dependent

pre-optimized collision energy and a collision energy shift mapping the −20 eV to +20 eV range in 2 eV steps in 21 separate runs. Hence, 21 different collision energy values for each peptide were measured, centered at a peptide specific default value, given by the following equation:

$$\text{collision energy (eV)} = 0.0368 \times (\text{precursor } m/z) + 4.2786$$

As part of the present work, collision energy dependent measurements of tryptic peptides were recorded on a Thermo Q-Exactive Focus Orbitrap mass spectrometer bearing an ESI source. UHPLC separation was performed on a Dionex 3000 UHPLC system. The experimental conditions were similar: in each run, 1 µg of HeLa digest was injected onto an Acquity BEH C-18 UPLC column (1.7 µm, 130 Å 1mm ×100 mm, Waters, Milford, MA, USA). Peptides were separated at 45°C using a flow rate of 100 µL/min. Solvent A consisted of water + 0.1% FA, while solvent B was acetonitrile + 0.1% FA. The gradient was as follows: 8% B from 0 to 1 min, followed by a 70 min gradient to 40% B, then the concentration of the solvent B was elevated to 80% in 1 min and kept there for 4 min. The ions were generated in positive ionization mode with the following source parameters: spray voltage was 3.5 kV, spray temperature was set to 320°C, sheath and auxiliary gas flows were kept 5 and 3 arbitrary units, respectively. The Q-Exactive Focus Orbitrap was operated as follows: full-scan MS spectra were acquired with a mass resolution of 35 000 using an ion target value of 3×10^6 (with maximum ion accumulation time of 100 ms) from m/z 350 to m/z 2000, followed by three sequential MS/MS scans using an ion target value of 1×10^5 (with ion accumulation time of 50 ms). Precursor selection was performed with a ±3.0 m/z isolation width. The minimum intensity threshold was set at 2×10^4. The normalized collision energy (NCE) of the MS/MS experiments was changed from 11 to 57% in steps of 2%, therefore 24 different

settings were measured in 24 separate LC-MS/MS runs. Note, the factory default NCE value is 27%. Conversion between NCE% and eV can be carried out with the equation:[33,34]

$$\text{collision energy (eV)} = \text{NCE (\%)} \times (\text{precursor } m/z) / 500 \times (\text{charge factor}).$$

The charge factor equals to 0.9 and 0.85 in the case of doubly and triply charged peptides, respectively. In order to overcome the run-to-run variability of the DDA measurements, three experimental series were taken, consisting of 69 LC-MS/MS runs altogether, and the collected data were merged.

The significantly different amount of HeLa digest (50 ng vs. 1 µg) injected in the case of the Bruker QTof and Thermo Orbitrap instruments is justified by the different sensitivity of the two LC-MS/MS systems. The major influencing factor is the difference between the variants of electrospray ionization source, being a nano-ESI source in the case of former and normal ESI source in the case of latter. Since the ionization efficiency of nano-ESI source outperforms that of the normal ESI source,[35–37] much smaller sample is required for the comparable analysis. The signal-to-noise ratios are similar in the two cases (see Figure 5), and the average of maximum Mascot scores differs only slightly (ca. 75 for QTof results and ca. 60 for Orbitrap results, see SI Table S1), confirming the appropriate choice of the sample amount.

Data Analysis

Similarity of leucine enkephalin and peptides from enolase spectra. The comparison of CID features on QTof and Orbitrap instruments, investigated on the leucine enkephalin peptide and enolase tryptic peptides, was performed using our previously published methodology.[26] Briefly, spectral comparison of tandem mass spectra was carried out in a pairwise manner and only peaks

with over 10% relative abundance at least for one collision energy on any of the instruments were included. The similarity was measured using the similarity index (SI), for which we adopted the frequently used definition as the dot product of the square root of the ion intensities in the spectra:[38–40]

$$\text{similarity index} = \frac{\sum_i \sqrt{x_i} \times \sqrt{y_i}}{\sqrt{(\sum_i x_i) \times (\sum_i y_i)}}$$

where x_i and y_i are intensities of the matching peaks in the two spectra under consideration (with x_i or y_i equal to zero if there is no match), and the sums go over all peaks in the spectra.

Similarity of QTof and HCD investigated on tryptic peptides from HeLa digest standard. The raw QTof data were first recalibrated using Bruker Compass DataAnalysis software 4.3 (Bruker Daltonik GmbH, Bremen, Germany) for the internal calibrant and MS/MS peak list generation was performed using ProteinScape software 3.1 (Bruker Daltonik GmbH, Bremen, Germany). The RawConverter software was applied to convert Orbitrap raw experimental files to mgf files.[41] MS/MS spectra taken on both instruments were searched against the human SwissProt database using the Mascot search engine version v2.5 (Matrix Science, London, U.K.). The common parameters were set as follows: trypsin as the enzyme, maximum two missed cleavages allowed, carbamidomethylation of cysteines as fixed modification, deamidation (N, Q), and oxidation (M) as variable modifications. The precursor mass tolerance was 7 ppm and 5 ppm, while fragment peak tolerance was 0.05 Da and 0.03 Da for QTof and Orbitrap measurements, respectively.[42] The resulting Mascot output files (.dat) were subject to further analysis by our recently developed program called Serac.[10]

In order to compare the fragmentation characteristics and energy dependence in QTof and Orbitrap mass spectrometers for large number of peptides, we tested the similarity between the MS/MS spectra acquired on the two instruments for a large set of tryptic peptides identified from the HeLa protein digest sample. Only fragment peaks which were annotated by the Mascot search engine were considered. This process served as a noise filter and helped us to grab the peaks relevant from proteomics point of view. Furthermore, since the precursor peak intensity was omitted in the experimental mgf files, only fragment intensities were involved in the analysis. Note that under typical proteomics experimental conditions, the parent peak intensity in the tandem mass spectra is low anyhow. These "annotated-fragment-based" similarity indices were calculated automatically from the Mascot output files using the Serac program and are referred to as SI_{frag} to highlight the difference from SI values discussed above.

Energy dependence of the identification (Mascot) score in the case of QTof experiments was already investigated in our earlier work.[8] The score vs. collision energy curves from the Orbitrap measurements were obtained and analyzed analogously and were compared for the two instruments at the peptide level (more details can be found in SI). Briefly, we first extracted the identification scores as a function of collision energy from the Mascot dat files. The score versus energy shift functions were then normalized by dividing all values with the maximum score for the given peptide ion. To ensure that we draw conclusions on the basis of confident peptide identifications, only those with a Mascot score over 15 were accepted. Furthermore, only those peptides were included in the energy dependent analysis that were found at least at three consecutive collision energies and that had a score over 25 in at least one case. For each peptide ion, the optimum energy was determined from the normalized score versus collision energy shift data sets by fitting one or two Gaussian functions. Two additional data points were added with

zero score outside the studied range, at ±35 eV collision energy shift and −8 NCE% and 62 NCE% for the QTof and Orbitrap experiments, respectively, to avoid erroneously wide peaks to be fitted. Where there were less than 12 data points in the original data, we only attempted to fit one Gaussian. Data for peptide ions with at least 12 points were fitted using both one and two Gaussian function and the two-peak fit was accepted if it provided a significantly better fit. The nonlinear fits were carried out, and the corresponding plots were generated using the levmar[43] and PGPLOT[44] libraries through their Perl Data Language interfaces. The positions of the center of the Gaussian peaks were considered as optimal values: a single energy value for one-peak fits (unimodal peptides) and two energy values for each two-peak fit (lower and higher energy optimum of the bimodal peptides).

RESULTS AND DISCUSSION

Comparison of QTof and Orbitrap HCD Using Leucine Enkephalin

Energy dependence of peptide fragmentation was studied both on the Thermo Orbitrap and on the Bruker Maxis QTof instruments. Like in our previous paper,[26] we used leucine enkephalin as the starting test compound, and the protonated molecule (MH^+, m/z = 556.2771) was studied. Its fragmentation is well understood;[32] formation of the major fragments occurs over a wide internal energy range. Therefore it seemed us a good choice to compare ion excitation in the different instruments. Example spectra at 20, 30 and 60 eV taken on the Bruker QTof instrument are shown on the left-hand side of Figure 1. The low energy fragments (like b_4 and a_4 ions) are formed at lower energy than that used for standard proteomics workflows (*e.g.*, see the 20 eV spectrum), while high energy fragments (like F and Y ions) become dominant at higher energy than that used for proteomics (*e.g.*, see the 60 eV spectrum). The right-hand side of Figure 1 depicts MS/MS

spectra acquired on the Thermo Orbitrap equipment at a collision energy setting providing the best similarity, i.e., giving the largest SI value, with the shown QTof MS/MS spectrum.

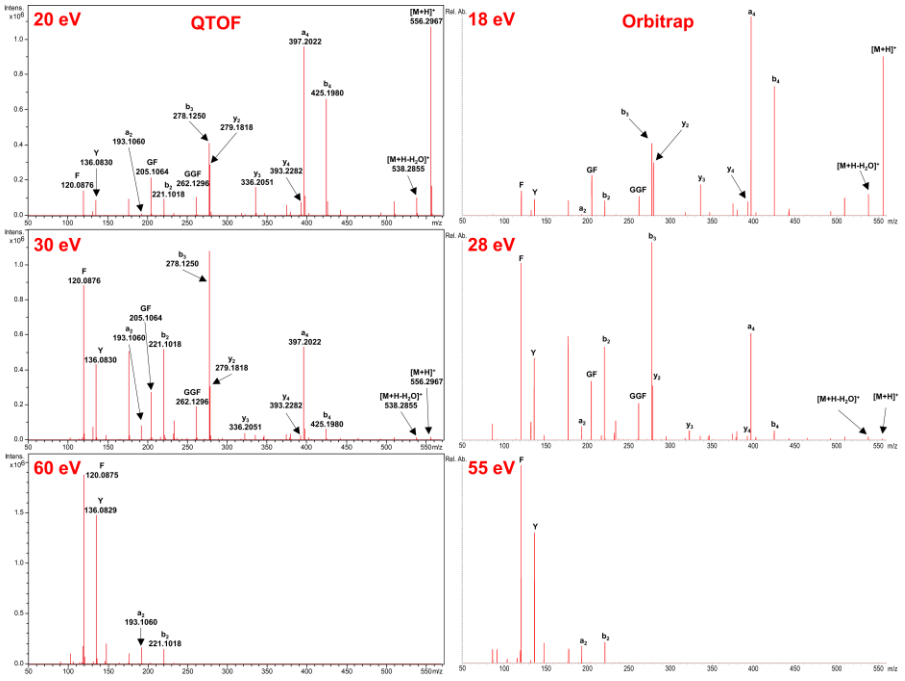

Figure 1. Selected examples of MS/MS spectra of leucine enkephalin recorded on the Bruker QTof instrument (left) and on the Thermo Orbitrap mass spectrometer (right). Spectra were taken at three different collision energies, namely at 20 eV, 30 eV and 60 eV in the case of QTof, and 18 eV, 28 eV and 55 eV in the case of Orbitrap-HCD. Collision energies of the Orbitrap MS/MS spectra for this Figure were chosen to provide the largest similarity index with the corresponding QTof MS/MS spectrum.

Spectra taken at various energies on the QTof and Orbitrap mass spectrometers were compared using the similarity index (see Experimental Section for more details); Figure 2a depicts a heat map of the similarity index as a function of the collision energies on the two instruments. At appropriate collision energies, excellent spectral similarities, in the range of 0.995-0.999, were obtained. This is a comparable degree of similarity to what was found between various QQQ and

QTof instruments, and only slightly worse than that of the reproducibility (0.999).[26] Collision energies giving similarity form a "ridge" in Figure 2a (dark red). To characterize the energy values on this ridge, for each energy setting on the QTof, we identified the energy setting yielding the highest similarity on the Orbitrap. For example, 38 eV on the QTof requires 35 eV on the Orbitrap for best match; these collision energy pairs are plotted in Figure 2b.

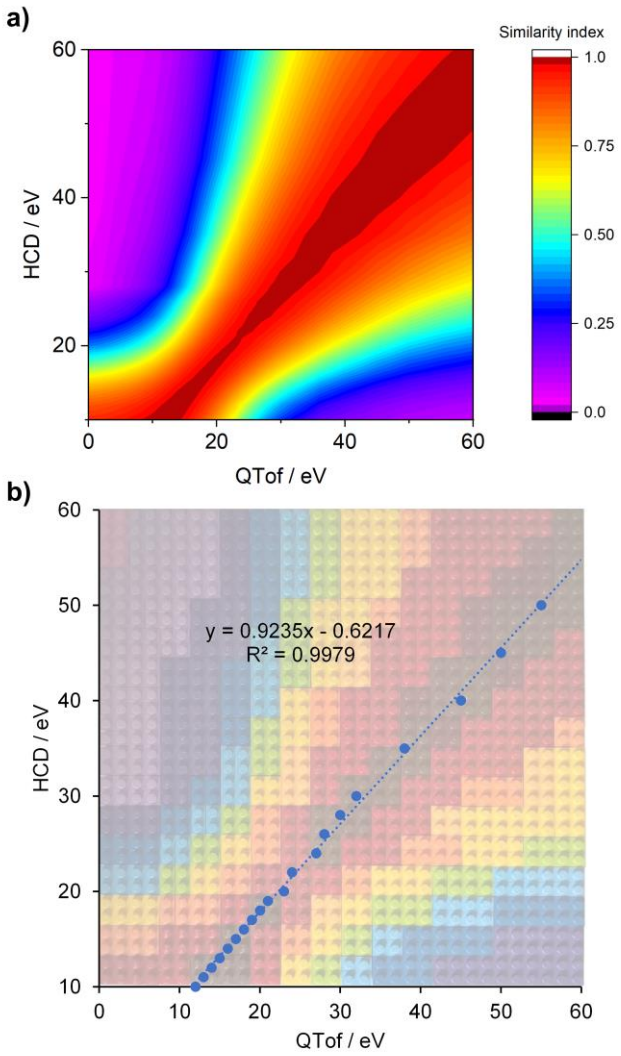

Figure 2. Similarity of tandem mass spectra of leucine enkephalin measured on Bruker QTof and Thermo Orbitrap mass spectrometers. (a) Heat map of similarity indices for all combinations of

collision energies and (b) collision energy pairs providing the best achievable similarity index, with a background of colored bricks to help recall the heat map of similarity indices.

Data in Figure 2b illustrate a strong linear relationship between the collision energy pairs corresponding to the ridge of the heat map. The linear fit is excellent (R^2=0.997), while the slope (0.92) is close, but clearly not equal to 1.0. This means that 1 eV increase in collision energy on the Thermo Orbitrap increases the internal energy of the precursor ion slightly more, than 1 eV increase on the Bruker QTof. The collision gas in both instruments is nitrogen, so this is not a center of mass effect. The difference might be due to a larger number of collisions in the Orbitrap (either due to higher collision gas pressure or longer collision cell), but we did not study this difference in detail.

The collision energy pairs presented in Figure 2b and the CE settings of matching MS/MS spectra presented on Figure 1 both demonstrate that the best similarity between the two instruments requires a few eV lower CE setting on the Orbitrap-HCD than on the QTof CID.

While spectral similarities between the spectra taken on the QTof and Orbitrap instruments are excellent, it might be important to highlight a major difference at low energy. In the case of the Orbitrap mass spectrometer, the lowest collision energy value that could be set is 10 eV. Spectra obtained at this energy is very similar to that obtained at 12 eV on the Bruker QTof (the survival yield is 84 and 85%, respectively). However, in the case of the Bruker QTof instrument it is possible to go down to as low as 0 eV, with a corresponding decrease in excitation. This is illustrated by the survival yield, which increase to 98% at 6 eV, ant to 99.4% at 0 eV. This difference may favor the Bruker QTof for the study of low stability compounds, like clusters, molecular complexes or phosphopeptides.

Comparison of QTof and Orbitrap HCD Using Tryptic Peptides from Enolase Standard

As a next step, we repeated the above experiments on representative examples of tryptic peptides. Two doubly charged and two triply charged peptides were chosen and mass-selected from the commercially available enolase tryptic digest standard. Investigations were performed on $NVNDVIAPAFVK^{2+}$ (m/z = 643.8546), $AVDDFLISLDGTANK^{2+}$ (m/z = 789.9048), $TAGIQIVADDLTVTNPK^{3+}$ (m/z = 585.9884) and $SIVPSGASTGVHEALEMR^{3+}$ (m/z = 614.3129) peptides. Their MS/MS spectra show fragments typical for tryptic peptide CID, namely, *y*-, *b*- and *a*-type ions, and their H_2O loss and NH_3 loss variants. The analysis of the acquired spectra was carried out analogously to that of leucine enkephalin. The resulting heat maps, as well as the linear fits of the CE settings providing best SI (see SI Figure S1-Figure S8) are fully in line with the above conclusions drawn from the study of leucine enkephalin peptide. High similarity between the QTof CID and Orbitrap-HCD spectra (SI 0.98-0.998 and 0.94-0.97 in the case of 2+ and 3+ peptides, respectively) could be achieved through the whole CE range, with a slightly lower CE setting on the Orbitrap-HCD than on the QTof CID.

Comparison of QTof and Orbitrap HCD Using Tryptic Peptides from HeLa Digest Standard

Similarity index

After investigating the leucine enkephalin reference compound, we compared QTof CID and Orbitrap HCD fragmentation from a proteomics point of view. First, we studied the CID and HCD MS/MS spectra of a large set of peptides identified from a HeLa tryptic digest sample. Spectra were recorded at various collision energies on both mass spectrometers. On the Bruker QTof equipment, 21 different collision energies were examined, mapping a 40 eV energy range. In total, 2152 peptides were identified in these runs, though not necessarily every peptide in every run (see

Table 1).[8] On the Thermo Orbitrap instrument, 24 different energy settings were investigated, covering a 46 NCE% range, and yielding 4277 identified peptides. When a given peptide was identified more than once at the same collision energy, i.e., it was measured several times either in the same LC−MS/MS run or in separate runs having the same collision energy setting, the best scoring match was accepted. To ensure a meaningful study, only peptide ions identified at least at three consecutive collision energy settings and having a minimum score of 25 at least at one of the energies on both mass spectrometers were considered for the MS/MS comparison study. These requirements left us with 1449 peptides; four-fifths of them were doubly charged, and most of the rest were triply charged, with a few examples for quadruply charged peptides (see Table 1). These species span the full hydrophobicity range typical for tryptic peptides (see retention time data in SI Table S1).

Table 1. Number of peptides with various properties identified from the Bruker QTof and Thermo Orbitrap experiments. QTof energy dependence results were taken from our earlier work.[8]

	QTof-CID	Orbitrap-HCD
Identified from all runs	2152	4277
Considered for energy dependence study	1721	3130
From this, 2+	1405	2014
From this, 3+	284	994
From this, unimodal fit	733	2573
From this, bimodal fit	988	557
Considered for comparison study	1449	1449
From this, 2+	1174	1174
From this, 3+	252	252
From this, unimodal fit	546	1057

From this, bimodal fit	903	392

The similarity of the MS/MS spectra recorded on the QTof and Orbitrap mass spectrometers was characterized by the similarity indices calculated from the annotated fragment ions (SI_{frag}, see Data Analysis). The indices were determined from the Mascot output files by our Serac program. Figure 3 depicts two examples, heat maps of the similarity index as a function of the collision energy for the TITLEVEPSDTIENVK^{2+} and ACANPAAGSVILLENLR^{2+} peptides. For various reasons (*e.g.*, larger step size in collision energy, complex sample, parent ion is not included, automatized data analysis) the results are not as smooth as in the case of leucine enkephalin (see above). Still the findings are qualitatively in line with those for the pure reference peptide. First, it can be seen that in order to achieve the highest similarity between the two fragmentation methods, the collision energy on the Thermo Orbitrap instrument has to be set to a lower value than on the Bruker QTof mass spectrometer by a few eV. For example, from the heat map of TITLEVEPSDTIENVK^{2+}, it is apparent that highest similarity to the setting of 50 eV on the QTof can be achieved by ~42 eV on the Orbitrap. Further, these SI_{frag} heat maps also corroborate that 1 eV higher setting on the Orbitrap mass spectrometer increases the energy of the parent ion by slightly more than a 1 eV higher setting on the QTof equipment does.

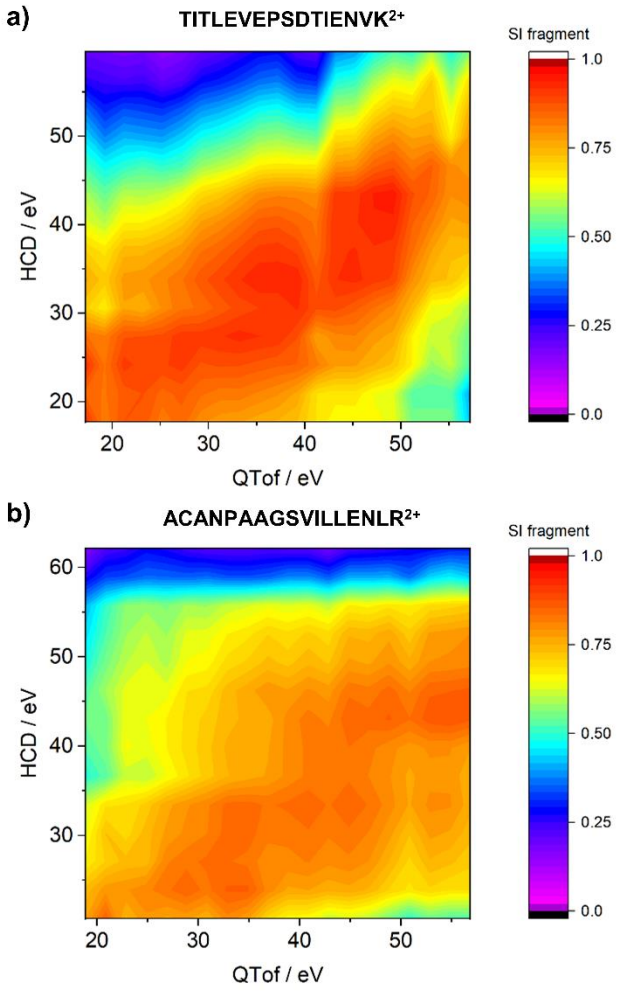

Figure 3. Similarity index heat maps from fragment ions (SI_{frag}) between QTof and HCD MS/MS spectra of peptides from proteomics measurements for (a) TITLEVEPSDTIENVK^{2+} and (b) ACANPAAGSVILLENLR^{2+} peptides as examples.

Mascot score vs. collision energy curves

Next, the collision energy dependence of Mascot score for tryptic peptides was examined. Analogously to our previous work focusing on the Bruker QTof experiments,[8] we created normalized Mascot score vs. collision energy curves for the Orbitrap HCD data. We processed 3130 peptides, ca. two-thirds of which were doubly charged and most of the rest were triply

charged (see Table 1). Similarly to the QTof CID results, three qualitatively different curve shapes were found; namely, a single, well-defined maximum; a broad plateau; or two well-defined peaks. We therefore modeled the data using one or two Gaussian functions, based on fit quality, and we refer to the cases as showing unimodal or bimodal behavior. The peak positions of the fits were considered to be the optimal collision energies (see below). In contrast to the QTof results, on the Orbitrap only a minority (ca. 20%) of the peptides showed bimodal behavior, i.e., showing either two maxima or a very broad peak due to the overlap of two Gaussians. Most peptides showed a simple, unimodal behavior.

As we discussed in our previous paper,[8] the bimodal behavior can be explained by the different energy dependence of the most important fragments, *y* and *b* ions. The *y* ions only show a slight dependence, with a weak tendency for a higher-energy optimum, while the *b* ions have clear preference for lower energies. Identification confidence is supported by both types of ions, leading to a broader range of favorable energies, or even two distinct peaks in the score vs. energy curve. The lower tendency for bimodal behavior in the case of Orbitrap measurements (see Table 1) might be explained by the smaller contribution of *b*-ion series in HCD spectra compared to CID spectra. We determined the maximum number of *b*-type ions through the covered collision energy range for the 1449 investigated peptides and on average CID spectra contained 60% more *b* ions (in terms of number of identified distinct peaks). Though the distinction between unimodal and bimodal curves is not clear-cut, we also tried to assess correlation of peptide properties with the unimodal/bimodal nature. We found that long peptides have a clear tendency to fall into the bimodal category, as demonstrated by the histograms of m/z values of unimodal and bimodal ions (see SI, Figure S11). Further, peptide ions containing mobile protons are bimodal significantly more often (80% bimodal) than peptides with only partially mobile ones (45% bimodal). This

finding is in line with the observation that the lower optimum energy for a mobile-proton containing bimodal peptide tends to be a few eV lower than that for the partially mobile ones, while the higher optimum energy of the two classes do not differ significantly.[8] We also investigated peptide properties like overall charge, presence of basic amino acids in the middle of the sequence, presence of K or R on the C-terminus, but these factors did not show any correlation with the bimodal behavior.

For the 1449 common peptides fulfilling the requirements of the energy dependence analysis on both instruments (see Table 1), we compared the score vs. collision energy curves for the individual peptides between the two fragmentation techniques. The curves are rather similar on the two instruments; Figure 4 depicts characteristic examples. The VLLPEYGGTK^{2+} peptide shows clear unimodal behavior on both instruments; the score maximum is at slightly lower collision energy (by 2.6 eV) in the case of the Orbitrap HCD experiments (Figure 4a). The curves of SLADELALVDVLEDK^{2+} peptide (Figure 4b) are practically identical at low energies, with optimum collision energy values also being close. At higher collision energies, a shoulder is observable in the QTof data, resulting in bimodal behavior, whereas unimodal behavior was found in the case of HCD fragmentation. This type of relationship is frequent and leads to the larger ratio of unimodal curves in the case of HCD method compared to CID technique (~20% vs. ~60%, see Table 1). Finally, the normalized score vs. collision energy curves of TITLEVEPSDTIENVK^{2+} peptide show bimodal behavior for both QTof and Orbitrap experiments (Figure 4c). Both maxima are at somewhat lower collision energies for the Orbitrap (7 and 8 eV in the case of lower and higher energy optimum, respectively); otherwise the curves are almost identical. In general, the energy dependence of normalized score values shows a high degree of similarity between the two

instruments, with lower optimum for HCD, which is in line with our findings from the analysis of similarity indices for leucine enkephalin and HeLa peptides.

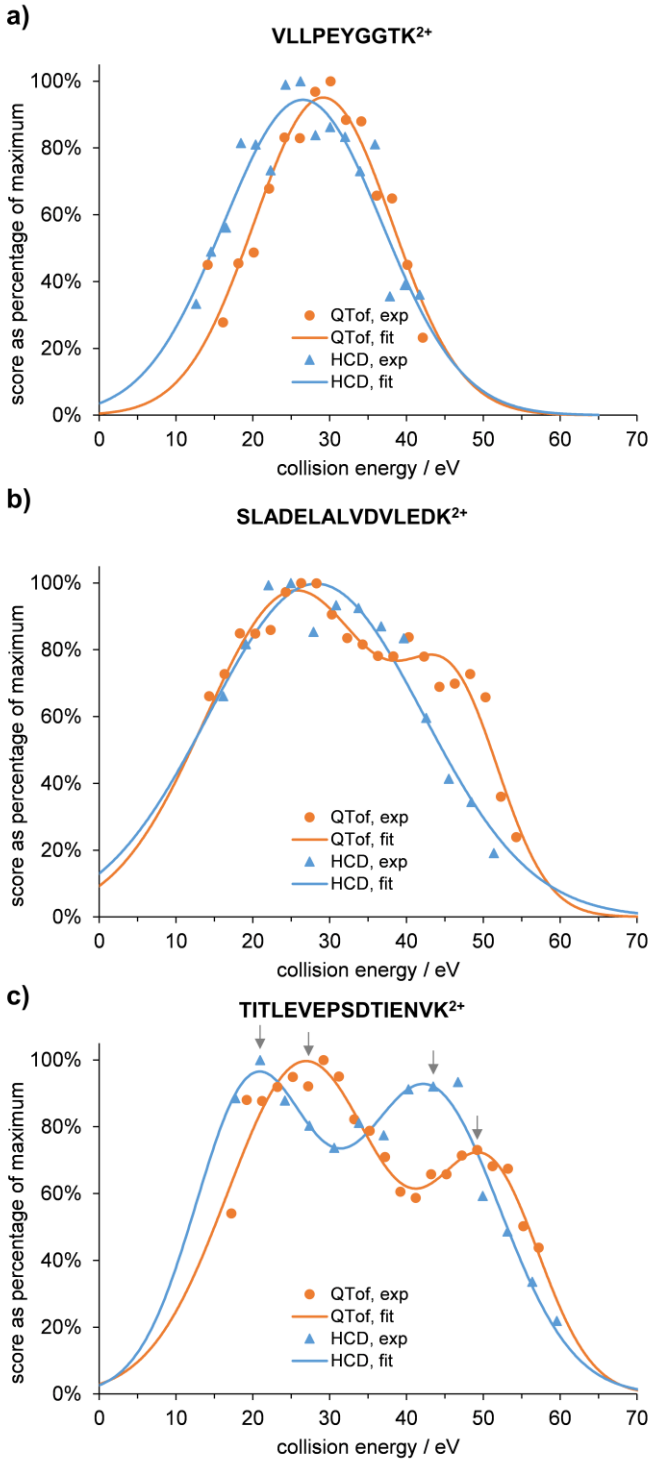

Figure 4. Result of fitting Gaussians to the energy dependence data points (score as % of the maximum value vs. collision energy in eV) of example peptides a) $VLLPEYGGTK^{2+}$, b) $SLADELALVDVLEDK^{2+}$ and c) $TITLEVEPSDTIENVK^{2+}$. Symbols denote measured data, while solid lines depict the one/two-Gaussian model functions. Blue/triangles and orange/squares depict Orbitrap HCD and QTof CID results, respectively. Grey arrows in subfigure c) indicate energies for which MS/MS spectra are presented (see later).

Figure 5 depicts the MS/MS spectra of $TITLEVEPSDTIENVK^{2+}$ peptide (having a bimodal behavior, Figure 4c) taken on the QTof and Orbitrap mass spectrometers at the collision energy setting closest to the Mascot score maxima (i.e., 27.2 eV and 49.2 eV for QTof, while 20.9 eV and 43.4 eV for Orbitrap measurements). The SI_{frag} values between CID and HCD spectra are 0.86 and 0.95 for the lower and higher energy maximum, respectively. Although these are smaller than that observed in the case of leucine enkephalin, the spectra recorded on the two different mass spectrometers are qualitatively very similar (Figure 5). The identity of most fragment ions and their abundance ratios agree quite well; the differences relate mostly to the presence or absence of some minor fragment ions. At the lower energy, *y* ions dominate the spectra, y_9, y_{10} and y_{11} being the most intense ones. Several *b* ions (b_5, b_6 and b_7) can be also found in the MS/MS spectra with relatively high intensity (Figure 5a-b). At the higher energy setting, the spectra are dominated by the y_9 ion in both cases, y_{10} and y_{11} are less prominent. As expected, *b* ions almost disappear,[7] b_3 and b_3–H_2O having the highest abundance (Figure 5c-d). This direct comparison of the spectra again confirms that the same information content can be achieved using QTof CID and Orbitrap HCD fragmentation technique if a proper CE adjustment is performed.

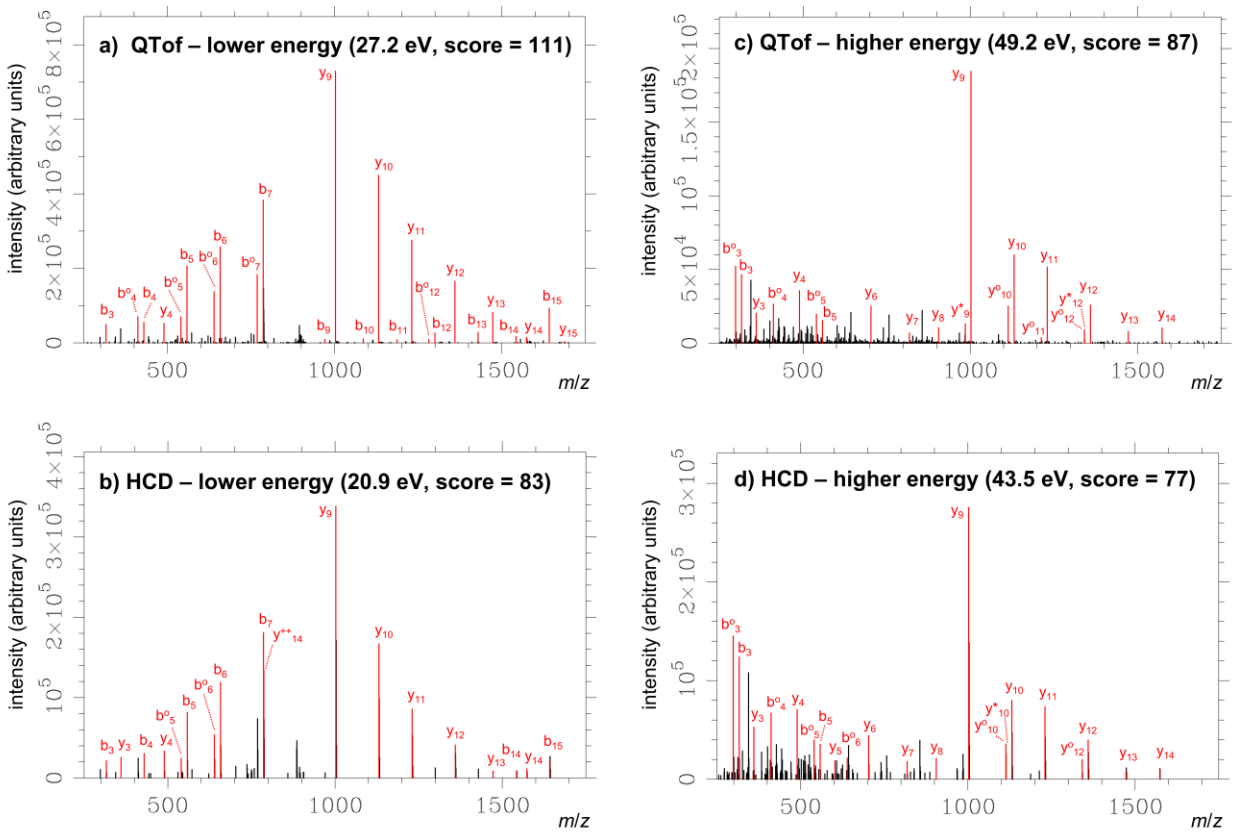

Figure 5. MS/MS spectra of the bimodal TITLEVEPSDTIENVK^{2+} peptide at the collision energy settings closest to the Mascot score maxima. a) and b), lower energy maximum on QTof and HCD; c) and d), higher energy maximum on QTof and HCD. The * superscript denotes NH_3 loss, while the ^{o} superscript denotes H_2O loss.

General trends on the optimal collision energy on Orbitrap-HCD

As a final step of our work, we moved the focus from the individual peptides to the general trends describing the full set of them. We determined the optimal CE values for the HCD experiments as the peak positions of the fitted Gaussian functions; one CE value for unimodal peptides and two CE value for bimodal ones. We plotted these optimum collision energies as a function of peptide ion *m*/*z* value. Results for doubly charged peptides are shown on Figure 6a. In this figure, optimum

energies from the unimodal fits are represented by blue circles, while grey and orange circles belong to the lower energy and higher energy optimum of bimodal peptides. Apparently, peak positions in each group follow linear trends with respect to *m*/*z* with relatively large R^2 values (see dashed lines). On Figure 6b, we present the same trend lines once again, together with those obtained for the QTof data from our earlier work.[8] It can be seen that the optimal CE as a function of *m*/*z* of the peptide is rather similar on the two instruments. The slopes are almost identical for the unimodal and lower bimodal part, and marginally different for the higher bimodal case. The major difference is that optimal settings are a few eV lower on the Orbitrap compared to the QTof instrument. We carried out a separate analysis for the triply charged peptides (see SI Figure S9 and Figure S10), which shows a broadly similar overall picture, with optimum energies being slightly lower as expected because of the higher charge, and the QTof - Orbitrap difference being somewhat smaller.

The above results on similarity and score-energy dependence are in line with the generally accepted view that fragmentation mechanisms are very similar in these two instruments.[45] While they do not perform identically per se, only minor differences in the ion internal energy distribution seem to be the reason, as collision energy tuning can bring them very close. Some differences in the energy distribution could stem from the ion source, ESI vs. nano-ESI in our case. Effects of (nano)ESI source design and settings on the energy have been extensively studied.[46–48] Most prominently, cone/skimmer voltages, but also capillary temperature and gas pressures may have an effect, just like droplet size and evaporation time, which are characteristically different for ESI and nano-ESI.[48] Still, it has been confirmed that under typical conditions, none of these effects is material. Concerning the ion transfer, the major difference between QTof-CID and Orbitrap-HCD is the presence of a C-trap, collecting precursor ions before activation in the latter case.[45] Further,

the time frame differs between QTof and Orbitrap instruments. The latter employs longer accumulation and trapping times, providing more time for the labile *b* ions to dissociate into smaller fragments (e.g., internal ions). This could be the reason for the somewhat lower number of *b* type ions in HCD spectra as compared to CID MS/MS. The ion activation also happens in somewhat different geometric arrangement. Still, our findings on spectrum similarity and peptide identification score-energy dependence confirm that the appropriate collision energy settings can ensure comparable proteomics performance of collision-induced dissociation methods, "be (it a) tof or be (it a) trap".[18]

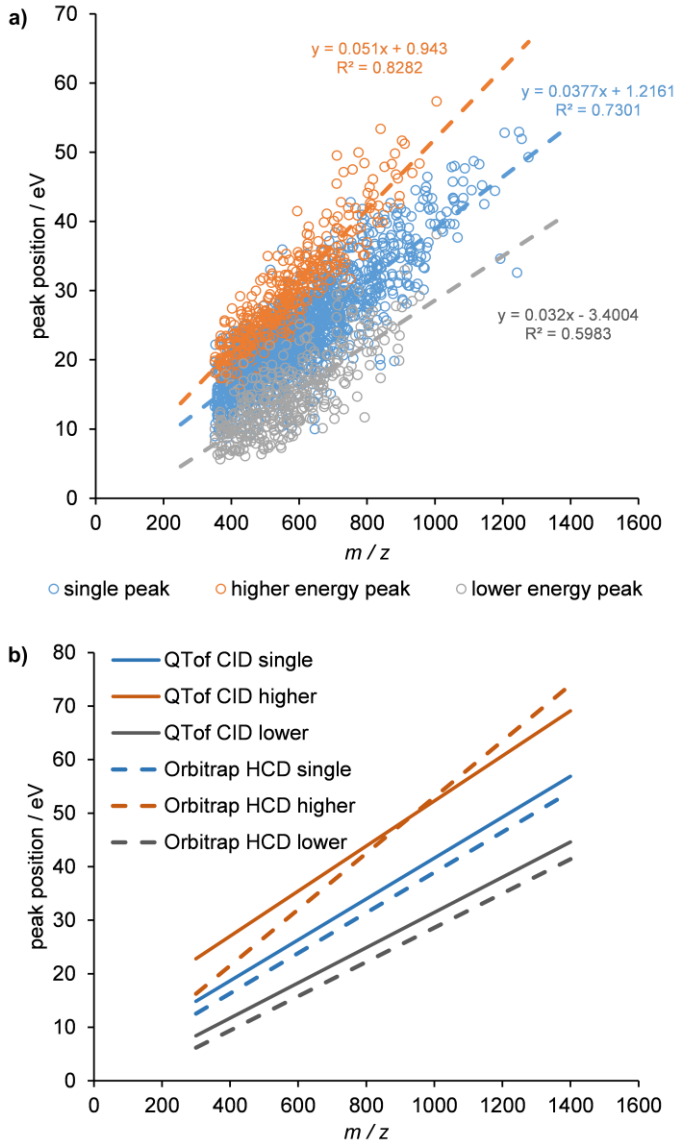

Figure 6. a) Peak positions in eV as a function of *m/z* for doubly charged peptides on the Orbitrap HCD. Blue circles indicate the position of the sole peak for peptides having unimodal behavior, while orange and grey circles are the higher and the lower collision energies, respectively, for bimodal peptides. Dashed lines represent linear fits**.** b) Linear fits to the optimal collision energy vs. *m/z* for doubly charged peptides on Orbitrap HCD (dashed lines; same as in the other subfigure) and QTof CID (solid lines). Blue, single optimum for unimodal peptides; orange, higher energy optimum for bimodal peptides; grey, lower energy optimum for bimodal peptides.

CONCLUSIONS

The CID on a QTof and the HCD on an Orbitrap are commonly considered equivalent in terms of MS/MS fragmentation characteristics, but to our knowledge, ours is the first study addressing this question in a systematic fashion by investigating a standard peptide (leucine enkephaline), a few tryptic peptides from a simple sample (enolase digest) and a complex peptide mixture (HeLa protein digest). We found that a proper adjustment of the collision energy is necessary, but that being ensured, very similar MS/MS spectra can indeed be obtained on the two instruments. Further, the energy dependence of peptide identification confidence ("score") shows comparable trends. Our results allowed us to the draw the following major conclusions:

1) The same collision energy setting produces somewhat more excitation in the Orbitrap HCD than in the QTof CID.

2) A slight (few eV) adjustment of the collision energy results in MS/MS spectra nearly identical using CID or HCD in a wide energy range.

3) In the configuration available to us, the Bruker QTof instrument is capable of generating 'colder' ions, than possible to obtain on the Orbitrap. This may be important for MS/MS analysis of very labile compounds.

4) Analysis of several thousand peptides shows that energy dependence of Mascot scores may have a narrow Gaussian, a wide Gaussian, or bimodal (two superposed Gaussian) shape. Occurrence of wide-Gaussian or bimodal distributions are more common in the case of the QTof, than on the Orbitrap.

5) Energy optimization for proteomics workflows shows that the two instruments behave very similarly in this respect. The optimum collision energy relates linearly to the m/z value of the precursor ion on both instruments.

Supporting Information. Single PDF file, containing details of the determination of the optimal collision energy, results on enolase peptides, a table of all investigated HeLa peptides, and results on triply charged peptides

Corresponding Author

* Ágnes Révész: revesz.agnes@ttk.hu, Phone: (+36-1) 382 6516

Funding Sources

Á.R. was supported by the János Bolyai Research Scholarship of the Hungarian Academy of Sciences. Funding from the National Research, Development and Innovation Office (NKFIH PD-132135 and K 131762) is gratefully acknowledged. G.S. acknowledges the support of the MTA Premium Post-Doctorate Research Program of the Hungarian Academy of Sciences (HAS, MTA). Purchase of the orbitrap mass spectrometer was supported by grant (VEKOP-2.3.3-15-2017-00020) from the European Union and the State of Hungary, co-financed by the European Regional Development Fund. Project no. 2018-1.2.1-NKP-2018-00005 has been implemented with the support provided from the National Research, Development and Innovation Fund of Hungary, financed under the 2018-1.2.1-NKP funding scheme.

REFERENCES

(1) Macias, L. A.; Santos, I. C.; Brodbelt, J. S. Ion Activation Methods for Peptides and Proteins. *Anal. Chem.* **2020**, *92*, 227–251. https://doi.org/10.1021/acs.analchem.9b04859.

(2) Sleno, L.; Volmer, D. A. Ion Activation Methods for Tandem Mass Spectrometry. *J. Mass Spectrom.* **2004**, *39* (10), 1091–1112. https://doi.org/10.1002/jms.703.

(3) Jennings, K. R. Analytical Applications of Ion Activation Techniques. *Int. J. Mass Spectrom.* **2015**, *377* (1), 610–616. https://doi.org/10.1016/j.ijms.2014.05.017.

(4) Paizs, B.; Suhai, S. Fragmentation Pathways of Protonated Peptides. *Mass Spectrom. Rev.* **2005**, *24*, 508–548. https://doi.org/10.1002/mas.20024.

(5) Lau, K. W.; Hart, S. R.; Lynch, J. A.; Wong, S. C. C.; Hubbard, S. J.; Gaskell, S. J. Observations on the Detection of B- and y-Type Ions in the Collisionally Activated Decomposition Spectra of Protonated Peptides. *Rapid Commun. Mass Spectrom.* **2009**, *23*, 1508–1514. https://doi.org/10.1002/rcm.4032.

(6) Waldera-Lupa, D. M.; Stefanski, A.; Meyer, H. E.; Stühler, K. The Fate of B-Ions in the Two Worlds of Collision-Induced Dissociation. *Biochim. Biophys. Acta - Proteins Proteomics* **2013**, *184*, 2843–2848. https://doi.org/10.1016/j.bbapap.2013.08.007.

(7) Holstein, C. A.; Gafken, P. R.; Martin, D. B. Collision Energy Optimization of B-and y-Ions for Multiple Reaction Monitoring Mass Spectrometry. *J. Proteome Res.* **2011**, *10*, 231–240. https://doi.org/10.1021/pr1004289.

(8) Révész, Á.; Rokob, T. A.; Jeanne Dit Fouque, D.; Turiák, L.; Memboeuf, A.; Vékey, K.; Drahos, L. Selection of Collision Energies in Proteomics Mass Spectrometry Experiments for Best Peptide Identification: Study of Mascot Score Energy Dependence Reveals Double Optimum. *J. Proteome Res.* **2018**, *17*, 1898–1906. https://doi.org/10.1021/acs.jproteome.7b00912.

(9) Révész, Á.; Milley, M. G.; Vékey, K.; Drahos, L. Tailoring to Search Engines: Bottom-up Proteomics with Collision Energies Optimized for Identification Confidence. submitted.

(10) Révész, Á.; Rokob, T. A.; Jeanne Dit Fouque, D.; Hüse, D.; Háda, V.; Turiák, L.; Memboeuf, A.; Vékey, K.; Drahos, L. Optimal Collision Energies and Bioinformatics Tools for Efficient Bottom-up Sequence Validation of Monoclonal Antibodies. *Anal. Chem.* **2019**. https://doi.org/10.1021/acs.analchem.9b03362.

(11) De Graaf, E. L.; Altelaar, M. A. F.; Van Breukelen, B.; Mohammed, S.; Heck, A. J. R. Improving SRM Assay Development: A Global Comparison between Triple Quadrupole, Ion Trap, and Higher Energy CID Peptide Fragmentation Spectra. *J. Proteome Res.* **2011**, *10*, 4334–4341. https://doi.org/10.1021/pr200156b.

(12) Wu, C.; Shi, T.; Brown, J. N.; He, J.; Gao, Y.; Fillmore, T. L.; Shukla, A. K.; Moore, R. J.; Camp, D. G.; Rodland, K. D.; et al. Expediting SRM Assay Development for Large-Scale Targeted Proteomics Experiments. *J. Proteome Res.* **2014**, *13*, 4479–4487. https://doi.org/10.1021/pr500500d.

(13) Cao, X.; Cai, X.; Mo, W. Comparing the Fragmentation Reactions of Protonated Cyclic Indolyl α-Amino Esters in Quadrupole/Orbitrap and Quadrupole Time-of-Flight Mass Spectrometers. *Rapid Commun. Mass Spectrom.* **2018**, *32* (7), 543–551. https://doi.org/10.1002/rcm.8063.

(14) Bade, R.; Rousis, N. I.; Bijlsma, L.; Gracia-Lor, E.; Castiglioni, S.; Sancho, J. V.; Hernandez, F. Screening of Pharmaceuticals and Illicit Drugs in Wastewater and Surface Waters of Spain and Italy by High Resolution Mass Spectrometry Using UHPLC-QTOF

MS and LC-LTQ-Orbitrap MS. *Anal. Bioanal. Chem.* **2015**, *407* (30), 8979–8988. https://doi.org/10.1007/s00216-015-9063-x.

(15) Glauser, G.; Veyrat, N.; Rochat, B.; Wolfender, J. L.; Turlings, T. C. J. Ultra-High Pressure Liquid Chromatography-Mass Spectrometry for Plant Metabolomics: A Systematic Comparison of High-Resolution Quadrupole-Time-of-Flight and Single Stage Orbitrap Mass Spectrometers. *J. Chromatogr. A* **2013**, *1292*, 151–159. https://doi.org/10.1016/j.chroma.2012.12.009.

(16) Abushareeda, W.; Tienstra, M.; Lommen, A.; Blokland, M.; Sterk, S.; Kraiem, S.; Horvatovich, P.; Nielen, M.; Al-Maadheed, M.; Georgakopoulos, C. Comparison of Gas Chromatography/Quadrupole Time-of-Flight and Quadrupole Orbitrap Mass Spectrometry in Anti-Doping Analysis: I. Detection of Anabolic-Androgenic Steroids. *Rapid Commun. Mass Spectrom.* **2018**, *32* (23), 2055–2064. https://doi.org/10.1002/rcm.8281.

(17) Kaufmann, A.; Walker, S. Comparison of Linear Intrascan and Interscan Dynamic Ranges of Orbitrap and Ion-Mobility Time-of-Flight Mass Spectrometers. *Rapid Commun. Mass Spectrom.* **2017**, *31* (22), 1915–1926. https://doi.org/10.1002/rcm.7981.

(18) Eichhorn, P.; Pérez, S.; Barceló, D. Time-of-Flight Mass Spectrometry Versus Orbitrap-Based Mass Spectrometry for the Screening and Identification of Drugs and Metabolites: Is There a Winner? *Compr. Anal. Chem.* **2012**, *58*, 217–272. https://doi.org/10.1016/B978-0-444-53810-9.00009-2.

(19) Saito-Shida, S.; Hamasaka, T.; Nemoto, S.; Akiyama, H. Multiresidue Determination of Pesticides in Tea by Liquid Chromatography-High-Resolution Mass Spectrometry:

Comparison between Orbitrap and Time-of-Flight Mass Analyzers. *Food Chem.* **2018**, *256* (February), 140–148. https://doi.org/10.1016/j.foodchem.2018.02.123.

(20) Duvivier, W. F.; van Beek, T. A.; Nielen, M. W. F. Critical Comparison of Mass Analyzers for Forensic Hair Analysis by Ambient Ionization Mass Spectrometry. *Rapid Commun. Mass Spectrom.* **2016**, *30* (21), 2331–2340. https://doi.org/10.1002/rcm.7722.

(21) Zhang, Y.; Yoshida, Y.; Xu, B.; Magdeldin, S.; Fujinaka, H.; Liu, Z.; Miyamoto, M.; Yaoita, E.; Yamamoto, T. Comparison of Human Glomerulus Proteomic Profiles Obtained from Low Quantities of Samples by Different Mass Spectrometry with the Comprehensive Database. *Proteome Sci.* **2011**, *9*, 1–11. https://doi.org/10.1186/1477-5956-9-47.

(22) Rose, R. J.; Damoc, E.; Denisov, E.; Makarov, A.; Heck, A. J. R. High-Sensitivity Orbitrap Mass Analysis of Intact Macromolecular Assemblies. *Nat. Methods* **2012**, *9* (11), 1084–1086. https://doi.org/10.1038/nmeth.2208.

(23) Reddy, P. J.; Ray, S.; Sathe, G. J.; Gajbhiye, A.; Prasad, T. S. K.; Rapole, S.; Panda, D.; Srivastava, S. A Comprehensive Proteomic Analysis of Totarol Induced Alterations in Bacillus Subtilis by Multipronged Quantitative Proteomics. *J. Proteomics* **2015**, *114*, 247–262. https://doi.org/10.1016/j.jprot.2014.10.025.

(24) Bantscheff, M.; Boesche, M.; Eberhard, D.; Matthieson, T.; Sweetman, G.; Kuster, B. Robust and Sensitive ITRAQ Quantification on an LTQ Obitrap Mass Spectrometer. *Mol. Cell. Proteomics* **2008**, *7* (9), 1702–1713. https://doi.org/10.1074/mcp.M800029-MCP200.

(25) Jang, I.; Lee, S. Y.; Hwangbo, S.; Kang, D.; Lee, H.; Kim, H. I.; Moon, B.; Oh, H. Bin. TEMPO-Assisted Free Radical-Initiated Peptide Sequencing Mass Spectrometry (FRIPS

MS) in Q-TOF and Orbitrap Mass Spectrometers: Single-Step Peptide Backbone Dissociations in Positive Ion Mode. *J. Am. Soc. Mass Spectrom.* **2017**, *28* (1), 154–163. https://doi.org/10.1007/s13361-016-1508-8.

(26) Bazsó, F. L.; Ozohanics, O.; Schlosser, G.; Ludányi, K.; Vékey, K.; Drahos, L. Quantitative Comparison of Tandem Mass Spectra Obtained on Various Instruments. *J. Am. Soc. Mass Spectrom.* **2016**, *27*, 1357–1365. https://doi.org/10.1007/s13361-016-1408-y.

(27) March, R. E. An Introduction to Quadrupole Ion Trap Mass Spectrometry. *J. Mass Spectrom.* **1997**, *32* (4), 351–369. https://doi.org/10.1002/(SICI)1096-9888(199704)32:4<351::AID-JMS512>3.0.CO;2-Y.

(28) McLuckey, S. A.; Goeringer, D. E. Slow Heating Methods in Tandem Mass Spectrometry. *J. Mass Spectrom.* **1997**, *32* (5), 461–474. https://doi.org/10.1002/(SICI)1096-9888(199705)32:5<461::AID-JMS515>3.0.CO;2-H.

(29) Graham Cooks, R.; Kaiser, R. E. Quadrupole Ion Trap Mass Spectrometry. *Acc. Chem. Res.* **1990**, *23* (7), 213–219. https://doi.org/10.1021/ar00175a002.

(30) Shao, C.; Zhang, Y.; Sun, W. Statistical Characterization of HCD Fragmentation Patterns of Tryptic Peptides on an LTQ Orbitrap Velos Mass Spectrometer. *J. Proteomics* **2014**, *109*, 26–37. https://doi.org/10.1016/j.jprot.2014.06.012.

(31) Michalski, A.; Neuhauser, N.; Cox, J.; Mann, M. A Systematic Investigation into the Nature of Tryptic HCD Spectra. *J. Proteome Res.* **2012**, *11* (11), 5479–5491. https://doi.org/10.1021/pr3007045.

(32) Sztáray, J.; Memboeuf, A.; Drahos, L.; Vékey, K. LEUCINE ENKEPHALIN—A MASS SPECTROMETRY STANDARD. *Mass Spectrom. Rev.* **2011**, *30* (2), 298–320. https://doi.org/10.1002/mas.20279.

(33) News in Proteomics Research, Proteomicsnews Blogpost http://proteomicsnews.blogspot.com/2014/06/normalized-collision-energy-calculation.html.

(34) Thermo Fisher Scientific Product Support Bulletin 104. Normalized Collision Energy Technology http://tools.thermofisher.com/content/sfs/brochures/PSB104-Normalized-Collision-Energy-Technology-EN.pdf.

(35) Emmett, M. R.; Caprioli, R. M. Micro-Electrospray Mass Spectrometry: Ultra-High-Sensitivity Analysis of Peptides and Proteins. *J. Am. Soc. Mass Spectrom.* **1994**, *5* (7), 605–613. https://doi.org/10.1016/1044-0305(94)85001-1.

(36) Gibson, G. T. T.; Mugo, S. M.; Oleschuk, R. D. Nanoelectrospray Emitters: Trends and Perspective. *Mass Spectrom. Rev.* **2009**, *28* (6), 918–936. https://doi.org/10.1002/mas.20248.

(37) Wilm, M. S.; Mann, M. Electrospray and Taylor-Cone Theory, Dole's Beam of Macromolecules at Last? *Int. J. Mass Spectrom. Ion Process.* **1994**, *136* (2–3), 167–180. https://doi.org/10.1016/0168-1176(94)04024-9.

(38) Tabb, D. L.; MacCoss, M. J.; Wu, C. C.; Anderson, S. D.; Yates, J. R. Similarity among Tandem Mass Spectra from Proteomic Experiments: Detection, Significance, and Utility. *Anal. Chem.* **2003**, *75* (10), 2470–2477. https://doi.org/10.1021/ac026424o.

(39) Wan, K. X.; Vidavsky, I.; Gross, M. L. Comparing Similar Spectra: From Similarity Index to Spectral Contrast Angle. *J. Am. Soc. Mass Spectrom.* **2002**, *13* (1), 85–88. https://doi.org/10.1016/S1044-0305(01)00327-0.

(40) Liu, J.; Bell, A. W.; Bergeron, J. J. M.; Yanofsky, C. M.; Carrillo, B.; Beaudrie, C. E. H.; Kearney, R. E. Methods for Peptide Identification by Spectral Comparison. *Proteome Sci.* **2007**, *5*, 1–12. https://doi.org/10.1186/1477-5956-5-3.

(41) He, L.; Diedrich, J.; Chu, Y. Y.; Yates, J. R. Extracting Accurate Precursor Information for Tandem Mass Spectra by RawConverter. *Anal. Chem.* **2015**, *87* (22), 11361–11367. https://doi.org/10.1021/acs.analchem.5b02721.

(42) Matrix Science, Mascot Search http://www.matrixscience.com/blog/back-to-basics-optimize-your-search-parameters.html#comments.

(43) Lourakis, M. I. A. Levmar: Levenberg-Marquardt Nonlinear Least Squares Algorithms in C/C++, Version 2.6. Institute of Computer Science, Foundation for Research and Technology – Hellas, Heraklion, Greece, http://www.ics.forth.gr/~lourakis/levmar/ 2011.

(44) Pearson, T. PGPLOT 5.2.2. California Institute of Technology, http://www.astro.caltech.edu/~tjp/pgplot/ 2001.

(45) Olsen, J. V.; Macek, B.; Lange, O.; Makarov, A.; Horning, S.; Mann, M. Higher-Energy C-Trap Dissociation for Peptide Modification Analysis. *Nat. Methods* **2007**, *4* (9), 709–712. https://doi.org/10.1038/nmeth1060.

(46) Gabelica, V.; De Pauw, E. Internal Energy and Fragmentation of Ions Produced in

Electrospray Sources. *Mass Spectrom. Rev.* **2005**, *24* (4), 566–587. https://doi.org/10.1002/mas.20027.

(47) Collette, C.; Drahos, L.; Pauw, E. De; Vékey, K. Comparison of the Internal Energy Distributions of Ions Produced by Different Electrospray Sources. *Rapid Commun. Mass Spectrom.* **1998**, *12* (22), 1673–1678. https://doi.org/10.1002/(SICI)1097-0231(19981130)12:22<1673::AID-RCM385>3.0.CO;2-A.

(48) Toubouly, D.; Jeckliny, M. C.; Zenobi, R. Ion Internal Energy Distributions Validate the Charge Residue Model for Small Molecule Ion Formation by Spray Methods. *Rapid Commun. Mass Spectrom.* **2008**, *22*, 1062–1068. https://doi.org/10.1002/rcm.3469.